

DiagnolLM: A Hybrid Bayesian Neural Language Framework for Interpretable Disease Diagnosis

Bowen Xu^{*1}, Xinyue Zeng^{*1},
Jiazen Hu¹, Tuo Wang¹, Adithya Kulkarni²

¹Department of Computer Science, Virginia Tech

²Department of Computer Science, Ball State University

Abstract

Building trustworthy clinical AI systems requires not only accurate predictions but also transparent, biologically grounded explanations. We present DiagnolLM, a hybrid framework that integrates Bayesian deconvolution, eQTL-guided deep learning, and LLM-based narrative generation for interpretable disease diagnosis. DiagnolLM begins with GP-unmix, a Gaussian Process-based hierarchical model that infers cell-type-specific gene expression profiles from bulk and single-cell RNA-seq data while modeling biological uncertainty. These features, combined with regulatory priors from eQTL analysis, power a neural classifier that achieves high predictive performance in Alzheimer’s Disease (AD) detection (88.0% accuracy). To support human understanding and trust, we introduce an LLM-based reasoning module that translates model outputs into audience-specific diagnostic reports, grounded in clinical features, attribution signals, and domain knowledge. Human evaluations confirm that these reports are accurate, actionable, and appropriately tailored for both physicians and patients. Our findings show that LLMs, when deployed as post-hoc reasoners rather than end-to-end predictors, can serve as effective communicators within hybrid diagnostic pipelines.

Introduction

Accurate disease diagnosis using transcriptomic data is a central goal in biomedical AI, yet it remains a formidable challenge due to two persistent bottlenecks: (1) the inability to extract cell-type-specific (CTS) signals from noisy bulk RNA-seq data, and (2) the lack of interpretable, clinically actionable explanations for model predictions. These limitations are especially pronounced in neurodegenerative diseases like Alzheimer’s Disease (AD), where pathology often manifests in specific brain cell types such as microglia and astrocytes (Blumenfeld et al. 2024; Brendel et al. 2022). Bulk RNA-seq, the most widely available data modality, aggregates expression over heterogeneous cell populations, thereby masking critical disease signals (Natri et al. 2024). Single-cell RNA-seq (scRNA-seq) offers higher resolution (Tasic et al. 2018; Paik et al. 2020; Yao et al. 2021), but its high cost, technical complexity, and sparsity in clinical cohorts make it impractical for widespread diagnostic use.

^{*}These authors contributed equally.

To bridge this gap, deconvolution methods have emerged that estimate CTS profiles from bulk RNA-seq using single-cell references (Xu et al. 2025). However, existing methods often fail to generalize due to their sensitivity to reference-target mismatch, lack of robust uncertainty modeling, and inability to propagate prior biological knowledge (Torroja and Sanchez-Cabo 2019). At the same time, most downstream disease classifiers treat gene expression purely as numerical input, ignoring known regulatory mechanisms such as expression quantitative trait loci (eQTLs) that offer causal, cell-type-aware insights into disease progression (Nica and Dermitzakis 2013; Natri et al. 2024). Even when accurate classifiers are developed, their “black-box” nature severely limits clinical adoption. Physicians and patients require not only predictions, but also clear, faithful explanations grounded in known biology (Blumenfeld et al. 2024). Recent work has explored the use of large language models (LLMs) in biomedical tasks (Yang et al. 2023; Gao et al. 2024; Han et al. 2022; Jiang, Zhang, and Xu 2025), yet most applications focus on end-to-end generation or information extraction. These approaches often lack alignment with underlying model behavior, leading to hallucinations and eroding trust in high-stakes settings (Omar et al. 2024; Chen, Luo, and Li 2025; Zhao et al. 2022; Zhang et al. 2024). Furthermore, LLMs exhibit well-documented limitations in handling symbolic reasoning and numerical precision (Hegselmann et al. 2023; Zhang et al. 2025; Hu et al. 2025), especially when used as primary decision-makers.

We argue that a reliable clinical AI system must unify three capabilities: robust signal extraction, biologically grounded prediction, and audience-specific explanation. To this end, we propose DiagnolLM, a hybrid neuro-symbolic framework for interpretable disease diagnosis. As shown in Figure 1, DiagnolLM integrates Bayesian deconvolution, regulatory genomics, and LLM-based explanation into a two-stage diagnostic pipeline. **Stage 1** introduces GP-unmix, a Gaussian Process-based hierarchical model that deconvolves bulk RNA-seq into CTS expression matrices using single-cell references. GP-unmix introduces posterior refinement steps to correct for reference-target shifts, incorporates uncertainty modeling via multivariate priors, and filters gene-cell-type pairs using biologically informed selection strategies. Compared to existing methods (Xu et al. 2025; Torroja and Sanchez-Cabo 2019), it achieves signif-

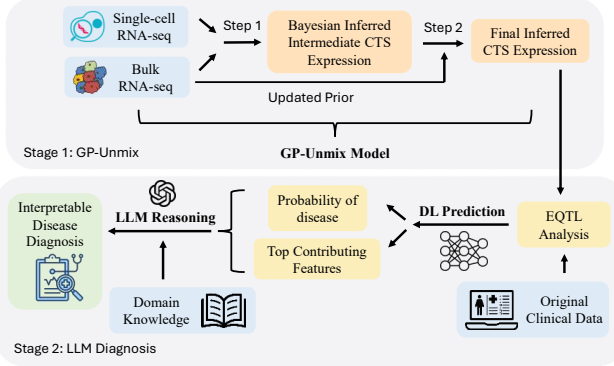


Figure 1: Overview of the DiagnolLM framework. Stage 1 (GP-Unmix) performs Bayesian deconvolution of bulk RNA-seq into CTS expression using single-cell references. Stage 2 combines eQTL-informed DL predictions with LLM-based reasoning to produce human-readable diagnostic reports, linking model outputs with clinical interpretability.

icantly higher gene-level recovery across tissues, species, and modalities. **Stage 2** enriches prediction with *eQTL-derived regulatory features* that guide a two-layer neural network classifier. These regulatory priors emphasize disease-relevant transcriptional mechanisms (Gusev et al. 2016; Natra et al. 2024), improving both classification performance (88.0% accuracy on AD) and biological alignment. To address the interpretability gap, we introduce a *language-based reasoning module*, where an LLM translates classifier outputs and feature attributions into structured, audience-specific diagnostic reports tailored for clinicians and patients. This module is grounded in attribution scores and domain knowledge, ensuring factual alignment and avoiding free-form hallucination (Yu et al. 2025).

We further justify this hybrid design through a targeted divergence analysis. We find that LLMs often misclassify samples with conflicting symbolic cues (e.g., a positive AD label with a negative BETA value), but outperform neural models in out-of-distribution regions by leveraging domain priors. Conversely, the MLP is more robust to statistical variance but fails in rare or extreme cases. This complementary behavior motivates our neuro-symbolic integration: the neural model handles structured prediction, while the LLM serves as a post-hoc communicator and narrative generator.

Our contributions are threefold:

- 1. GP-unmix for cell-type deconvolution:** A Bayesian framework with dynamic prior refinement and gene selection for uncertainty-aware recovery of CTS expression.
- 2. eQTL-guided neural prediction:** A classifier trained on deconvolved and regulatory features that demonstrates improved accuracy and mechanistic alignment in AD detection.
- 3. LLM-based explanation module:** A structured prompting system that generates clinically actionable reports, evaluated across user trust, rationale completeness, and audience-appropriateness.

DiagnolLM bridges probabilistic modeling, biological reasoning, and natural language explanation, offering a path forward for interpretable AI in real-world clinical diagnostics.

Related Work

CTS Estimation and Deconvolution Models. Cell-type-specific (CTS) expression estimation is critical for uncovering disease-relevant signals from heterogeneous tissue data. Traditional deconvolution approaches such as TCA and bMIND (Xu et al. 2025; Torroja and Sanchez-Cabo 2019) estimate CTS proportions using single-cell reference data, but often lack uncertainty modeling and fail to generalize across tissues or species. Our framework extends this line of work by introducing *GP-unmix*, a Bayesian model with dynamic posterior refinement and biologically grounded prior selection that produces uncertainty-aware CTS profiles.

LLMs for Disease Analysis. Large language models (LLMs) have increasingly been explored for biomedical tasks, including disease classification, literature summarization, and biomarker discovery (Yang et al. 2022; Levine et al. 2024; Zeng et al. 2025). Understanding disease-relevant cell types is essential for mechanistic modeling in complex conditions like Alzheimer’s Disease (Omar et al. 2024; Giuffrè et al. 2024). Advances in single-cell RNA-seq (Miranda et al. 2023; Mathys et al. 2019) and CTS analysis (Jagadeesh et al. 2022; Hampel et al. 1998) have enabled high-resolution disease modeling, but extracting insights from such data requires models that are both scalable and interpretable. Most existing LLM-based systems rely on pretraining to encode domain knowledge, but they often operate as black-box classifiers or free-form generators, limiting their reliability in clinical decision-making (Elsborg and Salvatore 2023).

LLMs for Cell-Type Annotation and Omics Reasoning. Recent work has integrated LLMs into single-cell workflows to automate cell-type annotation and improve reproducibility. scInterpreter (Li et al. 2024) uses LLMs to interpret scRNA-seq profiles, while the Single-Cell Omics Arena benchmark (Liu et al. 2024) evaluates LLM performance in multi-omics classification and cross-modality translation. These frameworks demonstrate LLMs’ potential to reduce manual burden in biological annotation tasks. However, such systems generally focus on stand-alone annotation rather than aligning explanations with structured model predictions or attribution signals, as we propose in DiagnolLM.

LLMs for Numerical and Tabular Reasoning. LLMs have also been adapted to handle structured numerical and tabular inputs. LIFT (Dinh et al. 2022) converts structured numerical data into natural language to enable LLMs like GPT-3 (Brown et al. 2020) and GPT-J (Wang and Komatsuzaki 2021) to perform classification and regression tasks with performance rivaling or surpassing conventional models. For nonlinear tasks, LIFT outperforms decision trees and deep MLPs, and for regression, it exceeds polynomial and nearest-neighbor methods. TabLLM (Hegselmann et al.

2023) extends this idea by using natural language serialization for zero- and few-shot classification, achieving competitive performance against strong ML baselines including logistic regression, XGBoost (Chen and Guestrin 2016), LightGBM (Ke et al. 2017), TabNet (Arik and Pfister 2021), and TabPFN (Hollmann et al. 2022), as well as foundation models like T0 (Sanh et al. 2021). To improve numeric precision, LUNA (Han et al. 2022) introduces numeric augmentations and representations (NumTok and NumBed) in transformer models such as BERT (Devlin et al. 2018) and RoBERTa (Liu et al. 2019). These enhancements allow LLMs to handle numeric inputs more faithfully, but challenges remain regarding symbolic overgeneralization and interpretability in real-world domains (Yang et al. 2023; Gao et al. 2024; Kulkarni et al. 2025). In addition to healthcare, LLMs for numerical reasoning have also been explored in finance (Ma et al. 2025; Zhu et al. 2024) and mathematical modeling (Schwartz et al. 2024; Lee et al. 2023), where grounding, consistency, and multi-step reasoning remain open challenges.

Unlike prior methods that employ LLMs as end-to-end predictors or annotation tools, DiagoLLM adopts a neuro-symbolic architecture that decouples numerical prediction from natural language explanation. The classifier is trained on biologically grounded features derived from Bayesian deconvolution and eQTL-informed priors (Nica and Dernitzakis 2013; Natri et al. 2024), ensuring mechanistic relevance. Meanwhile, the LLM functions as a structured reasoning module, guided by attribution scores and tailored to audience-specific interpretability goals. This hybrid design addresses a central gap in the literature: integrating LLMs into clinical pipelines not as autonomous decision-makers, but as faithful narrators of model behavior. While post-hoc interpretability tools such as SHAP and LIME are commonly used in clinical AI (Lundberg and Lee 2017; Ribeiro, Singh, and Guestrin 2016), they often lack biological context and are sensitive to perturbation artifacts. In contrast, DiagoLLM grounds its explanations in both domain knowledge and model saliency, enabling reliable, audience-aware diagnostic narratives.

Methodology

We present DiagoLLM, a modular framework that combines Bayesian deconvolution, regulatory reasoning, and LLM-based interpretation to enable accurate and interpretable disease diagnosis. It addresses bulk RNA-seq limitations by recovering cell-type-specific signals. We first define the problem, then detail each component.

Problem Statement

Let $X \in \mathbb{R}^{G \times N}$ denote a bulk RNA-seq gene expression matrix, where G is the number of genes and N is the number of patient samples. Each column $x_i \in \mathbb{R}^G$ represents a bulk gene expression profile that conflates signals from multiple cell types, thereby obscuring disease-relevant biological variation. Our objective is to develop a computational pipeline that, given X and auxiliary metadata (such as genotype and clinical covariates), can: (1) Estimate an

uncertainty-aware, cell-type-specific (CTS) expression tensor $Z \in \mathbb{R}^{G \times C \times N}$, where C is the number of cell types. CTS expression refers to the gene activity levels attributable to each individual cell type, which are not directly measurable in bulk RNA-seq, (2) Use these CTS representations in conjunction with expression quantitative trait loci (eQTLs), genetic variants that influence gene expression, to predict disease status (e.g., Alzheimer’s Disease), and (3) Produce natural language diagnostic reports that are aligned with model predictions and enriched with clinically relevant biological context, targeted at both physicians and patients.

This problem is especially challenging because (1) ground-truth CTS expression is not observed during training, (2) the influence of genetic variation on expression is often nonlinear and context-dependent, and (3) explanatory outputs must be both accurate and understandable to diverse users.

The DiagoLLM Framework

To address the limitations of bulk RNA-seq in capturing cell-type-specific signals, the need for biologically grounded prediction, and the demand for interpretable clinical outputs, we propose DiagoLLM—a modular neuro-symbolic framework that integrates Bayesian deconvolution, regulatory reasoning, and structured language-based interpretation. Unlike prior approaches that treat LLMs as end-to-end predictors, DiagoLLM separates statistical inference from explanation: a neural classifier predicts disease status using features derived from Bayesian deconvolution and eQTL priors, while an LLM generates post-hoc, audience-specific diagnostic narratives. The framework is guided by three core principles: (1) extracting fine-grained molecular signals from noisy data, (2) grounding predictions in validated regulatory features, and (3) enabling transparent, clinically relevant explanations.

Specifically, DiagoLLM tackles the three key modeling challenges as follows: (1) To disentangle confounded expression signals, we introduce a Bayesian deconvolution module called GP-unmix, which infers gene-level expression profiles at the resolution of individual cell types. The method leverages sc/snRNA-seq references and employs a two-stage posterior refinement strategy to adapt to domain shifts between reference and target data. (2) To improve predictive accuracy and biological specificity, we incorporate known genetic regulatory variation in the form of eQTL priors. These priors are combined with CTS expression and clinical covariates to train a compact neural classifier that predicts Alzheimer’s Disease (AD) status, and (3) To promote trust and usability, we use a large language model (LLM) as a post-hoc reasoning module that generates human-readable diagnostic reports. These reports are grounded in model attributions and tailored for different audiences (e.g., physicians or patients). Figure 1 provides an overview of the full pipeline. Below, we describe each of the three components in detail.

Bayesian Deconvolution via GP-unmix

Motivation. A key obstacle in analyzing bulk RNA-seq is that it conflates gene expression across diverse cell

types, thereby masking cell-type-specific (CTS) transcriptional programs that may be crucial for disease mechanisms. For instance, Alzheimer’s related dysregulation in astrocytes or microglia may be diluted in bulk measurements dominated by neuronal signatures. Existing deconvolution methods, such as bMIND and TCA (Xu et al. 2025; Torroja and Sanchez-Cabo 2019), focus primarily on estimating cell-type proportions and lack the ability to recover full gene-level CTS expression with robust uncertainty quantification. Moreover, they often fail under domain shifts, such as differences in species, tissue, or sequencing protocols between reference and target datasets.

GP-unmix is a hierarchical Bayesian model designed to address these challenges. It infers CTS expression matrices from bulk data by combining: (1) multivariate priors derived from single-cell RNA-seq references, (2) posterior refinement to adapt to cohort-specific distributions, and (3) a tripartite gene selection strategy to improve stability and biological relevance.

Model Formulation. Let $X \in \mathbb{R}^{G \times N}$ denote the bulk RNA-seq matrix of G genes and N patient samples. The latent CTS expression tensor is denoted by $Z \in \mathbb{R}^{G \times C \times N}$, where C is the number of cell types. For each gene g and cell type j , we model CTS expression across samples as:

$$Z_{gj} \sim \mathcal{N}(\mu_j, \Sigma_j), \quad X_i = w_i^\top Z_i + \Gamma_j^\top C_i^{(1)} + w_i^\top B_j C_i^{(2)} + \varepsilon_i$$

Here, $w_i \in \mathbb{R}^C$ denotes the cell-type proportions for sample i ; $C_i^{(1)}$ captures bulk-level technical covariates such as batch effects; $C_i^{(2)}$ represents latent confounders at the cell-type-specific (CTS) level; Γ_j and B_j are learned adjustment matrices that modulate the influence of these covariates; and $\varepsilon_i \sim \mathcal{N}(0, \sigma_j^2)$ denotes the observation noise.

Reference-Informed Inference. We initialize priors (μ_j, Σ_j) using mean and covariance statistics from sc/snRNA-seq references (e.g., Tasic (Tasic et al. 2018), Yao (Yao et al. 2021)). These empirical distributions anchor the generative model and provide biologically grounded starting points.

Posterior Refinement. To accommodate domain shifts between references and target cohorts, we update the priors using posterior samples:

$$\mu_j^{(2)} \sim \mathcal{N}(\widehat{\mu_j^{(1)}}, \tau^2 I), \quad \Sigma_j^{(2)} \sim \text{InvWishart}(\widehat{\Sigma_j^{(1)}}, v)$$

Inference is performed via MCMC sampling with convergence validated using Gelman–Rubin diagnostics ($\hat{R} < 1.05$). We summarize the posterior inference process in Algorithm 1.

Tripartite Gene Selection. We reduce inference noise by selecting informative gene–cell-type pairs through three filters: 1. *Core markers*: manually curated genes known to mark specific cell types (e.g., *SLC6A12*, *C3*), 2. *Statistical stability*: differentially expressed genes across modalities ($p_{\text{FDR}} < 0.01$, $|\log_2 \text{FC}| > 1$), and 3. *Noise suppression*: filtering based on Seurat-derived differential expression scores. This selection strategy improves downstream

CTS estimation, yielding 37–54% higher Pearson correlation coefficients (PCC) compared to baselines across multiple datasets, especially in low-abundance or high-noise cell populations.

Algorithm 1: GP-unmix: Posterior Inference

Require: Bulk RNA-seq matrix X , reference dataset \mathcal{R} , covariates $C^{(1)}, C^{(2)}$

- 1: Initialize priors $(\mu_j^{(0)}, \Sigma_j^{(0)})$ from \mathcal{R}
- 2: Select gene–cell-type pairs using tripartite gene filtering
- 3: **for** each pair (g, j) **do**
- 4: Draw samples: $Z_{gj}^{(1)} \sim \mathcal{N}(\mu_j^{(0)}, \Sigma_j^{(0)})$
- 5: **end for**
- 6: Fit bulk mixture: $X_i \approx w_i^\top Z_i + \Gamma_j^\top C_i^{(1)} + w_i^\top B_j C_i^{(2)}$
- 7: Estimate posteriors $(\widehat{\mu_j^{(1)}}, \widehat{\Sigma_j^{(1)}})$
- 8: Update priors and repeat MCMC sampling for T iterations
- 9: **Return** Posterior means $\mathbb{E}[Z_{gj} \mid X]$, variances $\text{Var}[Z_{gj} \mid X]$

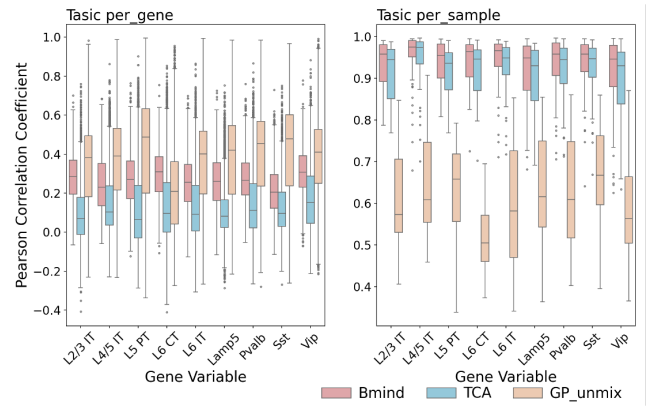


Figure 2: GP-unmix improves CTS recovery over TCA and bMIND across neuron subtypes in the Tasic dataset (Tasic et al. 2018).

Empirical Validation. Figures 2 and 3 benchmark GP-unmix on the Tasic and Yao datasets, respectively. It achieves higher Pearson correlation than bMIND and TCA at both per-gene and per-sample levels, particularly on complex and low-abundance populations such as L6 CT, Lamp5, and Pvalb interneurons. In human brain data, GP-unmix achieves a median PCC of 0.82 for microglia and 0.78 for astrocytes. In PBMCs, it yields strong alignment with flow cytometry ground-truth ($r = 0.71$ for NK cells), outperforming bMIND by over 105%. These CTS profiles enable downstream regulatory analysis. In the ROSMAP Alzheimer’s cohort, GP-unmix reveals astrocyte-linked dysregulation in UDP-glucosyltransferase activity, a pathway implicated in neurodegenerative inflammation, thus demonstrating both predictive utility and biological interpretability.

eQTL-Guided Disease Classification

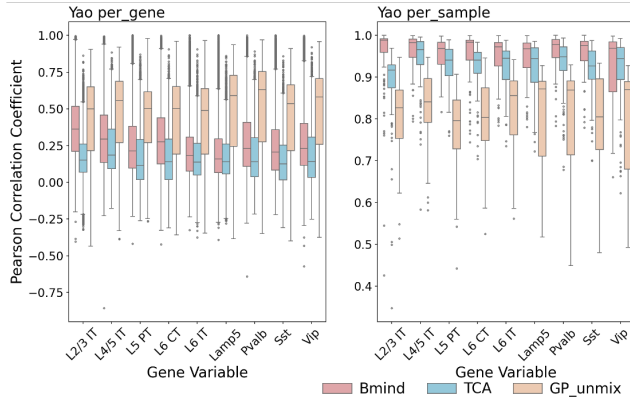


Figure 3: GP-unmix outperforms baselines on astrocytes, microglia, and inhibitory subtypes in the Yao dataset (Yao et al. 2021).

Motivation. While CTS expression inferred by GP-unmix provides granular transcriptional features, not all expression variability is biologically meaningful or disease-relevant. Expression quantitative trait loci (eQTLs), genetic variants that modulate gene expression in a cell-type-specific manner, offer mechanistic priors that ground observed expression shifts in underlying regulatory architecture. Incorporating these priors enables the classifier to prioritize biologically plausible features and reduce reliance on noise or confounding signals, particularly in complex disorders like Alzheimer’s Disease (AD).

Feature Construction. Each patient sample is represented using a concatenation of three biologically motivated components: 1. *CTS expression vectors*: Mean expression values for selected gene-cell-type pairs output by GP-unmix, 2. *eQTL-derived regulatory priors*: For each gene, we include effect size (BETA), uncertainty (SE), and statistical significance (PVAL), obtained from cohort-specific or public databases, and 3. *Covariates*: Demographic and technical confounders such as age, sex, and batch indicators. These vectors are standardized and projected into a compact, biologically grounded feature space for classification.

Classifier Design. We implement a two-layer feedforward neural network (MLP) trained using binary cross-entropy loss. The model includes ReLU activations, dropout regularization, and early stopping based on validation loss. The simplicity of this architecture is intentional to ensure transparency and compatibility with gradient-based attribution methods.

Attribution and Interpretability. To enable post-hoc explanation via LLMs, we compute feature attributions using Integrated Gradients. These attributions, indicating the contribution of each input feature to the model’s output, serve as intermediate representations for structured diagnostic narrative generation in the next stage of the pipeline.

LLM-Based Diagnostic Interpretation

Motivation. Despite advances in disease classification accuracy, clinical deployment requires models to produce explanations that are understandable, faithful, and tailored to different stakeholders. LLMs offer a promising solution by translating structured model outputs into human-readable reports. However, when used as standalone predictors, LLMs often lack numerical grounding and exhibit inconsistency in reasoning. We address this by using the LLM as a post-hoc interpretability module, conditioned on model outputs, feature attributions, and biomedical priors, to generate explanations aligned with both statistical evidence and clinical knowledge.

Input Representation. The LLM receives as input a structured prompt composed of: 1. *Predicted label and confidence*: Binary AD prediction and associated softmax probability from the classifier, 2. *Feature attributions*: Saliency scores from Integrated Gradients, reflecting which CTS expression and eQTL features influenced the model’s decision, and 3. *Biological priors*: Contextual information on key genes (e.g., *APOE*, *TREM2*) derived from public literature or cohort-specific findings. These components are serialized into natural language using prompt templates, enabling compatibility with standard instruction-tuned LLMs such as GPT-3.5 or BioMedLM.

Prompting Strategies. We experiment with three progressively structured prompting approaches: 1. *Direct Reasoning*: The LLM receives a flattened list of features and is asked to output a diagnosis label with minimal guidance. 2. *Step-by-Step Reasoning*: The LLM first summarizes distributions of features across known AD and non-AD populations, then compares the test case against these learned distributions before making a decision. 3. *Step-by-Step with Domain Knowledge*: The prompt is augmented with biomedical background (e.g., known AD gene signatures), encouraging the LLM to reason using established clinical knowledge alongside the model’s attributions.

Audience-Specific Report Generation. Using the same internal representation, the LLM is prompted to generate diagnostic narratives tailored to two user groups: 1. *Clinician reports*: Emphasize biomarker relevance, statistical confidence, and biological pathways involved, and 2. *Patient summaries*: Simplify terminology and focus on actionable insights while preserving factual fidelity. These reports help close the loop between high-performance predictive modeling and real-world interpretability demands in precision medicine.

LLM as Post-hoc Interpretability Module

While LLMs can occasionally outperform deep learning models in low-data settings, their use as end-to-end classifiers in clinical contexts is risky due to sensitivity to heuristics and lack of numerical rigor. In DiagnolLM, we instead deploy the LLM as a post-hoc interpretability module, conditioned on outputs from a statistically trained neural model. This design ensures predictive stability while enabling transparent and audience-aligned explanation.

Each LLM-generated report is prompted with: (a) the MLP-predicted probability $p(\text{AD})$, and (b) the top-5 most influential features determined by Integrated Gradients, including feature values, attribution scores, and reference ranges. The LLM is then prompted to output: (1) a binary decision (yes/no for AD), (2) a rationale grounded in feature-level reasoning, and (3) next-step recommendations (e.g., clinical follow-up, lifestyle guidance). We generate two versions per report: one for clinicians (technical terms and differential risk framing) and one for patients (plain language with actionable summaries).

Experiments

We evaluate DIAGNOLLM’s hybrid architecture across three fronts: (1) LLM prompting vs. deep learning baselines, (2) divergence analysis of LLM and MLP behaviors, and (3) expert assessments of explanation quality.

Classification Setup and Baseline Comparison

We evaluate LLM prompting strategies for binary Alzheimer’s Disease (AD) classification on a structured clinical dataset containing 28 features per patient, including biomarkers, vitals, and genetic markers. Two training regimes are considered: *low-data* (50 training samples) and *full-data* (100 training samples), both evaluated on a fixed held-out test set of 100 randomly-sampled samples to ensure consistent comparison.

As a structured baseline, we implement a two-layer multi-layer perceptron (MLP) trained on the same feature set. The MLP comprises two fully connected layers (input \rightarrow 16 \rightarrow 8 \rightarrow 1) with ReLU activations, followed by a sigmoid output for binary prediction. The model is trained using the Adam optimizer (learning rate = 0.001) with binary cross-entropy (BCE) loss. The LLM used in our study is GPT-4o-mini.

Table 1 summarizes classification performance across all methods. The MLP achieves the highest accuracy in the full-data setting, but underperforms the LLM in the low-data regime when domain knowledge is incorporated. The structured prompt with domain guidance (**LLM+Domain**) achieves 90% accuracy and 0.89 F1, surpassing the MLP by 3 points, underscoring the utility of knowledge-informed prompting in data-scarce medical contexts.

Method	Train Size = 100		Train Size = 50	
	ACC	F1	ACC	F1
MLP (DL)	0.88	0.86	0.87	0.88
LLM-Direct	0.48	0.43	0.50	0.49
LLM-Step	0.70	0.62	0.77	0.75
LLM+Domain	0.74	0.69	0.90	0.89

Table 1: Classification accuracy and F1 across prompting variants and MLP baseline under different data regimes.

Divergence Analysis of LLM and MLP Reasoning

While our quantitative results highlight the benefits of combining deep learning with structured prompting, this section offers deeper insight into DiagnOLLM’s hybrid design.

Specifically, we compare the behavioral failure modes of the MLP and LLM components to justify why we treat the LLM as a post-hoc reasoner rather than a standalone classifier.

Symbol-Sensitive Failures in LLMs LLMs tend to apply overly rigid rules when interpreting symbolic patterns, such as associating the sign of BETA with class labels. We curated a test subset of 100 Alzheimer’s-positive (AD) samples with negative BETA values, along with corresponding SE and PVAL¹, to evaluate LLM behavior under symbolic conflicts. On this diagnostic subset, the LLM achieved only 38.71% accuracy, compared to the MLP’s 89.19%. Manual inspection revealed that the LLM often ignored the uncertainty (SE) or statistical significance (PVAL), leading to heuristic overfitting.

Out-of-Distribution Magnitude Failures in MLPs In contrast, the MLP underperforms on test samples with feature values outside the training distribution. We constructed a subset of 100 such outlier instances with at least one feature exceeding $\pm 1\sigma$ from the training mean. On this set, the MLP accuracy dropped to 61.26%, while the LLM, leveraging biomedical priors, reached 88.00%. These results underscore the MLP’s fragility in sparse data regimes and the LLM’s generalization via conceptual knowledge.

Case Studies of Model Divergence To illustrate the above patterns, we present three representative cases in Table 2. Each example reveals a distinct strength or failure mode and supports the use of a hybrid structure combining MLP precision with LLM transparency.

Case	Features	Label	MLP	LLM	Key Insight
1: LLM Er- ror	BETA = -0.03185; SE = 0.04911; PVAL = 0.51671	AD	AD	non- AD	LLM applies rigid rule to BETA sign; ig- nores uncertainty and p-value.
2: MLP Er- ror	BETA = 0.976; SE = 0.571; PVAL = 2.166	AD	non- AD	AD	MLP misclas- sifies due to extreme input; LLM leverages domain priors.
3: Agree- ment	BETA = 0.041; SE = 0.061; PVAL = 0.436	AD	AD	AD	LLM offers ex- plicit rationale tied to BETA range; MLP is opaque.

Table 2: Examples of divergence and complementarity between MLP and LLM in AD classification.

These results validate our architectural choice: the MLP provides stable decision-making grounded in statistical learning, while the LLM augments transparency and robustness via biomedical priors. Used as a post-hoc reasoning engine, the LLM mitigates model brittleness and enables ex-

¹BETA denotes the effect size of an eQTL on gene expression, SE is its standard error, and PVAL indicates the associated statistical significance.

planatory alignment with human reasoning, critical for real-world adoption in clinical settings.

LLM-Guided Interpretation: Case Studies and Evaluation

While LLMs have shown promise in low-data regimes, their use as standalone clinical classifiers remains limited by symbolic rigidity and poor numerical grounding. DiagnolLM instead adopts a hybrid strategy: the LLM functions purely as a post-hoc interpretability module, translating neural model outputs into structured, audience-specific diagnostic narratives. This separation ensures predictive reliability while enhancing transparency through saliency-aware, domain-grounded explanation.

We now present two representative case studies to illustrate how the LLM explanations reflect biological plausibility and align with known Alzheimer’s Disease (AD) mechanisms.

Patient A: High-Risk APOE Carrier

- **Summary:** APOE-positive, $p(\text{AD}) = 0.83$, Final decision: AD
- **Key Features:** Elevated triglycerides (220.78 mg/dL), low albumin, poor diet, and high creatinine—all well-established risk factors amplified in APOE carriers (Hunsberger et al. 2019).
- **Model Alignment:** MLP prioritizes lipids and inflammation; LLM weaves these into a narrative with recommendations for lipid management and neuroimaging.

Patient B: Low-Risk APOE Non-Carrier

- **Summary:** APOE-negative, $p(\text{AD}) = 0.10$, Final decision: non-AD
- **Key Features:** Age (80.37), elevated homocysteine (16.26 $\mu\text{mol/L}$), LDL cholesterol (111.93 mg/dL), and short sleep duration (5 hours).
- **Model Alignment:** MLP flags vascular and metabolic markers with moderate weights. LLM offers a conservative explanation, advising monitoring and lifestyle adjustments.

These examples demonstrate the explanatory alignment between the LLM outputs and model attributions, as well as their grounding in established AD biology. They highlight the utility of DiagnolLM in producing audience-specific, biologically coherent diagnostic reports that support real-world clinical communication.

Simulated User Study on Trust and Explanation Quality

To assess the real-world utility of our interpretability module, we conducted a simulated user study focused on how structured, audience-specific LLM-generated reports are perceived by human experts. The study involved raters with clinical training, who evaluated the trustworthiness, clarity, and actionability of diagnostic reports across two audience types: physicians and laypersons.

Evaluation Design We sampled 60 explanation reports (30 clinician-facing and 30 patient-facing) and asked three expert raters to independently score each report across five qualitative dimensions: 1. *Prediction Agreement*: Does the rater agree with the model’s decision? 2. *Feature Rationale*: Are key predictive features explicitly referenced? 3. *Actionability*: Are meaningful next steps (e.g., lifestyle changes, follow-ups) suggested? 4. *Justification Coherence*: Is the explanation logically connected to the outcome? 5. *Stylistic Fit*: Is the tone appropriate for the target audience?

Evaluation Dimension	Agreement Comment (%)
Prediction	100.0
Agreement	Raters accepted all decisions
Feature Rationale	45.0
Actionability	Attribution often underspecified
Justification	94.2
Coherence	Logical flow needs refinement
Stylistic Fit	17.5
	Generally well-matched tone

Table 3: Expert ratings across explanation dimensions (n=60 reports).

Results Summary As Table 3 shows, all reports aligned with model decisions, but only 45% referenced key features, and fewer than 20% offered clear evidence-to-conclusion reasoning. Still, 94.2% were rated actionable, and 76.7% were appropriately styled for their target audience.

Illustrative Examples

- **Patient A (Physician Report):** Correct decision, but cited only “age” as rationale despite stronger drivers. Justification was vague, but next steps and tone were appropriate.
- **Patient B (Layperson Report):** Correct diagnosis, but explanation contained technical terms (“LDL,” “homocysteine”), making it less accessible.
- **Patient C (Physician Report):** Strong alignment across all dimensions—clear reasoning, feature-based rationale, appropriate language.

These findings confirm that DiagnolLM produces actionable, trusted explanations, but also reveal weaknesses in feature attribution and logical coherence. These results underscore the need for stronger prompt grounding and closer integration between model interpretation and generation.

Conclusion

We present DiagnolLM, a modular diagnostic framework that unifies Bayesian deconvolution, genetic regulatory modeling, and LLM-based interpretability to address key challenges in clinically grounded, cell-type-aware disease prediction. Our proposed *GP-unmix* model recovers uncertainty-aware, cell-type-specific gene expression with

high fidelity, substantially outperforming existing deconvolution approaches across species and tissues. By integrating these expression profiles with eQTL priors, a deep learning classifier, and structured language model prompts, DiAGNOLLM achieves robust prediction performance alongside transparent, audience-specific explanations. Through detailed divergence analysis, biological case studies, and a simulated user study, we demonstrate that our hybrid design mitigates the symbolic rigidity of LLMs and the numerical fragility of neural predictors, offering interpretability without sacrificing performance.

References

Arik, S. Ö.; and Pfister, T. 2021. Tabnet: Attentive interpretable tabular learning. In *Proceedings of the AAAI conference on artificial intelligence*, volume 35, 6679–6687.

Blumenfeld, J.; Yip, O.; Kim, M. J.; and Huang, Y. 2024. Cell type-specific roles of APOE4 in Alzheimer disease. *Nature Reviews Neuroscience*, 25(2): 91–110.

Brendel, M.; Su, C.; Bai, Z.; Zhang, H.; Elemento, O.; and Wang, F. 2022. Application of deep learning on single-cell RNA sequencing data analysis: a review. *Genomics, proteomics & bioinformatics*, 20(5): 814–835.

Brown, T.; Mann, B.; Ryder, N.; Subbiah, M.; Kaplan, J. D.; Dhariwal, P.; Neelakantan, A.; Shyam, P.; Sastry, G.; Askell, A.; et al. 2020. Language models are few-shot learners. *Advances in neural information processing systems*, 33: 1877–1901.

Chen, T.; and Guestrin, C. 2016. Xgboost: A scalable tree boosting system. In *Proceedings of the 22nd ACM SIGKDD international conference on knowledge discovery and data mining*, 785–794.

Chen, Z.; Luo, X.; and Li, D. 2025. VisRL: Intention-Driven Visual Perception via Reinforced Reasoning. *arXiv:2503.07523*.

Devlin, J.; Chang, M.-W.; Lee, K.; and Toutanova, K. 2018. BERT: Pre-training of Deep Bidirectional Transformers for Language Understanding. *arXiv preprint arXiv:1810.04805*.

Dinh, T.; Zeng, Y.; Zhang, R.; Lin, Z.; Gira, M.; Rajput, S.; Sohn, J.-y.; Papailiopoulos, D.; and Lee, K. 2022. Lift: Language-interfaced fine-tuning for non-language machine learning tasks. *Advances in Neural Information Processing Systems*, 35: 11763–11784.

Elsborg, J.; and Salvatore, M. 2023. Using LLM Models and Explainable ML to Analyse Biomarkers at Single Cell Level for Improved Understanding of Diseases. *bioRxiv*, 2023–08.

Gao, Y.; Myers, S.; Chen, S.; Dligach, D.; Miller, T. A.; Bitterman, D.; Churpek, M.; and Afshar, M. 2024. When Raw Data Prevails: Are Large Language Model Embeddings Effective in Numerical Data Representation for Medical Machine Learning Applications? *arXiv preprint arXiv:2408.11854*.

Giuffrè, M.; Kresevic, S.; Pugliese, N.; You, K.; and Shung, D. L. 2024. Optimizing large language models in digestive disease: strategies and challenges to improve clinical outcomes. *Liver International*, 44(9): 2114–2124.

Gusev, A.; Ko, A.; Shi, H.; Bhatia, G.; Chung, W.; Pennington, B. W.; Jansen, R.; De Geus, E. J.; Boomsma, D. I.; Wright, F. A.; et al. 2016. Integrative approaches for large-scale transcriptome-wide association studies. *Nature genetics*, 48(3): 245–252.

Hampel, H.; Teipel, S. J.; Alexander, G. E.; Horwitz, B.; Teichberg, D.; Schapiro, M. B.; and Rapoport, S. I. 1998. Corpus callosum atrophy is a possible indicator of region-and cell type-specific neuronal degeneration in Alzheimer disease: A magnetic resonance imaging analysis. *Archives of neurology*, 55(2): 193–198.

Han, H.; Xu, J.; Zhou, M.; Shao, Y.; Han, S.; and Zhang, D. 2022. LUNA: language understanding with number augmentations on transformers via number plugins and pre-training. *arXiv preprint arXiv:2212.02691*.

Hegselmann, S.; Buendia, A.; Lang, H.; Agrawal, M.; Jiang, X.; and Sontag, D. 2023. Tabllm: Few-shot classification of tabular data with large language models. In *International Conference on Artificial Intelligence and Statistics*, 5549–5581. PMLR.

Hollmann, N.; Müller, S.; Eggensperger, K.; and Hutter, F. 2022. Tabpfn: A transformer that solves small tabular classification problems in a second. *arXiv preprint arXiv:2207.01848*.

Hu, M.; Wang, J.; Zhao, W.; Zeng, Q.; and Luo, L. 2025. FlowMalTrans: Unsupervised Binary Code Translation for Malware Detection Using Flow-Adapter Architecture. *arXiv:2508.20212*.

Hunsberger, H. C.; Pinky, P. D.; Smith, W.; Suppiramaniam, V.; and Reed, M. N. 2019. The role of APOE4 in Alzheimer’s disease: strategies for future therapeutic interventions. *Neuronal signaling*, 3(2): NS20180203.

Jagadeesh, K. A.; Dey, K. K.; Montoro, D. T.; Mohan, R.; Gazal, S.; Engreitz, J. M.; Xavier, R. J.; Price, A. L.; and Regev, A. 2022. Identifying disease-critical cell types and cellular processes by integrating single-cell RNA-sequencing and human genetics. *Nature genetics*, 54(10): 1479–1492.

Jiang, F.; Zhang, Z.; and Xu, X. 2025. CMFDNet: Cross-Mamba and Feature Discovery Network for Polyp Segmentation. *arXiv:2508.17729*.

Ke, G.; Meng, Q.; Finley, T.; Wang, T.; Chen, W.; Ma, W.; Ye, Q.; and Liu, T.-Y. 2017. Lightgbm: A highly efficient gradient boosting decision tree. *Advances in neural information processing systems*, 30.

Kulkarni, A.; Alotaibi, F.; Zeng, X.; Wu, L.; Zeng, T.; Yao, B. M.; Liu, M.; Zhang, S.; Huang, L.; and Zhou, D. 2025. Scientific Hypothesis Generation and Validation: Methods, Datasets, and Future Directions. *arXiv:2505.04651*.

Lee, N.; Sreenivasan, K.; Lee, J. D.; Lee, K.; and Papailiopoulos, D. 2023. Teaching arithmetic to small transformers. *arXiv preprint arXiv:2307.03381*.

Levine, D.; Rizvi, S. A.; Lévy, S.; Pallikkavallyaveetil, N.; Zhang, D.; Chen, X.; Ghadermarzi, S.; Wu, R.; Zheng, Z.; Vrkic, I.; et al. 2024. Cell2Sentence: teaching large language models the language of biology. *bioRxiv*, 2023–09.

Li, C.; Xiao, M.; Wang, P.; Feng, G.; Li, X.; and Zhou, Y. 2024. scInterpreter: Training Large Language Models to Interpret scRNA-seq Data for Cell Type Annotation. *arXiv preprint arXiv:2402.12405*.

Liu, J.; Xu, S.; Zhang, L.; and Zhang, J. 2024. Single-Cell Omics Arena: A Benchmark Study for Large Language Models on Cell Type Annotation Using Single-Cell Data. *arXiv:2412.02915*.

Liu, Y.; Ott, M.; Goyal, N.; Du, J.; Joshi, M.; Chen, D.; Levy, O.; Lewis, M.; Zettlemoyer, L.; and Stoyanov, V. 2019. RoBERTa: A Robustly Optimized BERT Pretraining Approach. *arXiv preprint arXiv:1907.11692*.

Lundberg, S. M.; and Lee, S.-I. 2017. A unified approach to interpreting model predictions. *Advances in neural information processing systems*, 30.

Ma, T.; Du, J.; Huang, W.; Wang, W.; Xie, L.; Zhong, X.; and Zhou, J. T. 2025. Llm knows geometry better than algebra: Numerical understanding of llm-based agents in a trading arena. *arXiv preprint arXiv:2502.17967*.

Mathys, H.; Davila-Velderrain, J.; Peng, Z.; Gao, F.; Mohammadi, S.; Young, J. Z.; Menon, M.; He, L.; Abdurrob, F.; Jiang, X.; et al. 2019. Single-cell transcriptomic analysis of Alzheimer's disease. *Nature*, 570(7761): 332–337.

Miranda, A. M.; Janbandhu, V.; Maatz, H.; Kanemaru, K.; Cranley, J.; Teichmann, S. A.; Hübner, N.; Schneider, M. D.; Harvey, R. P.; and Noseda, M. 2023. Single-cell transcriptomics for the assessment of cardiac disease. *Nature Reviews Cardiology*, 20(5): 289–308.

Natri, H. M.; Del Azodi, C. B.; Peter, L.; Taylor, C. J.; Chugh, S.; Kendle, R.; Chung, M.-i.; Flaherty, D. K.; Matlock, B. K.; Calvi, C. L.; et al. 2024. Cell-type-specific and disease-associated expression quantitative trait loci in the human lung. *Nature Genetics*, 56(4): 595–604.

Nica, A. C.; and Dermitzakis, E. T. 2013. Expression quantitative trait loci: present and future. *Philosophical Transactions of the Royal Society B: Biological Sciences*, 368(1620): 20120362.

Omar, M.; Brin, D.; Glicksberg, B.; and Klang, E. 2024. Utilizing natural language processing and large language models in the diagnosis and prediction of infectious diseases: A systematic review. *American Journal of Infection Control*.

Paik, D. T.; Cho, S.; Tian, L.; Chang, H. Y.; and Wu, J. C. 2020. Single-cell RNA sequencing in cardiovascular development, disease and medicine. *Nature Reviews Cardiology*, 17(8): 457–473.

Ribeiro, M. T.; Singh, S.; and Guestrin, C. 2016. "Why should i trust you?" Explaining the predictions of any classifier. In *Proceedings of the 22nd ACM SIGKDD international conference on knowledge discovery and data mining*, 1135–1144.

Sanh, V.; Webson, A.; Raffel, C.; Bach, S. H.; Sutawika, L.; Alyafeai, Z.; Chaffin, A.; Stiegler, A.; Scao, T. L.; Raja, A.; et al. 2021. Multitask prompted training enables zero-shot task generalization. *arXiv preprint arXiv:2110.08207*.

Schwartz, E.; Choshen, L.; Shtok, J.; Doveh, S.; Karlinsky, L.; and Arbelle, A. 2024. NumeroLogic: Number Encoding for Enhanced LLMs' Numerical Reasoning. *arXiv preprint arXiv:2404.00459*.

Tasic, B.; Yao, Z.; Graybuck, L. T.; Smith, K. A.; Nguyen, T. N.; Bertagnolli, D.; Goldy, J.; Garren, E.; Economo, M. N.; Viswanathan, S.; et al. 2018. Shared and distinct transcriptomic cell types across neocortical areas. *Nature*, 563(7729): 72–78.

Torroja, C.; and Sanchez-Cabo, F. 2019. Digitaldsorter: deep-learning on scRNA-Seq to deconvolute gene expression data. *Frontiers in Genetics*, 10: 978.

Wang, B.; and Komatsuzaki, A. 2021. GPT-J-6B: A 6 Billion Parameter Autoregressive Language Model. <https://github.com/kingoflolz/mesh-transformer-jax>.

Xu, X.; Li, R.; Mo, O.; Liu, K.; Li, J.; and Hao, P. 2025. Cell-type deconvolution for bulk RNA-seq data using single-cell reference: a comparative analysis and recommendation guideline. *Briefings in Bioinformatics*, 26(1): bbaf031.

Yang, F.; Wang, W.; Wang, F.; Fang, Y.; Tang, D.; Huang, J.; Lu, H.; and Yao, J. 2022. scBERT as a large-scale pretrained deep language model for cell type annotation of single-cell RNA-seq data. *Nature Machine Intelligence*, 4(10): 852–866.

Yang, Z.; Mitra, A.; Liu, W.; Berlowitz, D.; and Yu, H. 2023. TransformEHR: transformer-based encoder-decoder generative model to enhance prediction of disease outcomes using electronic health records. *Nature communications*, 14(1): 7857.

Yao, Z.; Liu, H.; Xie, F.; Fischer, S.; Adkins, R. S.; Aldridge, A. I.; Ament, S. A.; Bartlett, A.; Behrens, M. M.; Van den Berge, K.; et al. 2021. A transcriptomic and epigenomic cell atlas of the mouse primary motor cortex. *Nature*, 598(7879): 103–110.

Yu, X.; Hu, X.; Wan, X.; Zhang, Z.; Wan, X.; Cai, M.; Yu, T.; and Xiao, J. 2025. A unified framework for cell-type-specific eQTL prioritization by integrating bulk and scRNA-seq data. *The American Journal of Human Genetics*, 112(2): 332–352.

Zeng, X.; Wang, T.; Kulkarni, A.; Lu, A.; Ni, A.; Xing, P.; Zhao, J.; Chen, S.; and Zhou, D. 2025. DISPROTBENCH: A Disorder-Aware, Task-Rich Benchmark for Evaluating Protein Structure Prediction in Realistic Biological Contexts. *arXiv:2507.02883*.

Zhang, Y.; Chen, Q.; Zhou, J.; Wang, P.; Si, J.; Wang, J.; Lu, W.; and Qin, L. 2024. Wrong-of-Thought: An Integrated Reasoning Framework with Multi-Perspective Verification and Wrong Information. *arXiv:2410.04463*.

Zhang, Y.; Liu, X.; Tao, R.; Chen, Q.; Fei, H.; Che, W.; and Qin, L. 2025. ViTCoT: Video-Text Interleaved Chain-of-Thought for Boosting Video Understanding in Large Language Models. *arXiv:2507.09876*.

Zhao, Z.; Zhai, Y.; Chen, B. M.; and Liu, P. 2022. BALF: Simple and Efficient Blur Aware Local Feature Detector. *arXiv:2211.14731*.

Zhu, F.; Liu, Z.; Feng, F.; Wang, C.; Li, M.; and Chua, T. S. 2024. TAT-LLM: A Specialized Language Model for Discrete Reasoning over Financial Tabular and Textual Data. In

Proceedings of the 5th ACM International Conference on AI in Finance, 310–318.